Fe₃Al Iron Aluminides Alloyed with High Concentrations of V and Cr: Their Structure and High Temperature Strength

PETR KRATOCHVÍL, STANISLAV DANIŠ, JOSEF PEŠIČKA, PETER MINÁRIK, and ROBERT KRÁL

Eight iron aluminide alloys with different contents of V and Cr were prepared up to 25 at. pct of both elements. The effect of the V and Cr concentration on the microstructure and mechanical properties was investigated by several complementary techniques. This investigation revealed that the microstructure of all the investigated alloys was comparable regardless of their chemical composition. All the alloys were in a solid solution condition without any major chemical inhomogeneity. For all alloys, a comparable grain size and $D0_3$ crystallographic structure was observed. *In situ* X-ray diffraction measurement revealed that the crystallographic structure was stable up to 1073 K (800 °C) regardless of the chemical composition. Mechanical testing showed that the compressive yield stress significantly increased with the increasing total sum of V plus Cr. Much higher values of yield stress were measured for symmetric concentrations of V and Cr when compared to non-symmetric ones. Eventually, it was shown that the formation of at least a rough system of the lattice positions occupation by four types of atoms in four sub-lattices derived from $D0_3$ is the most probable strengthening factor for alloys with symmetric concentrations of V and Cr.

I. INTRODUCTION

REGARDLESS of the intensive research on different iron-based materials, alloys based on iron aluminides remain ideal candidates for the development of new structural materials with improved performance in petrochemical, power-generation, and aeronautical applications.[1,2] The major advantages of iron aluminides are excellent resistance to oxidation and sulfidation, a high strength-to-weight ratio (two-thirds of the density of steel), high electrical resistance, and the input material is relatively inexpensive due to the high content of Fe and Al. The high strength-to-weight ratio of this material and chemical stability is particularly useful for industrial applications. Nevertheless, the main drawbacks of these alloys strongly limit their wider utilization—particularly their poor workability at room temperature and low high-temperature (HT) strength. Huge efforts have been made to increase the HT strength of iron aluminides and now a variety of methods have been developed, see, *e.g.*, References 3 and 4. The most common ones are based on alloying and are, in particular,

- Strengthening by solid solution hardening (SSH)—typically Cr, Mo, or V.[4,5]
- Strengthening by $D0_3$ order increase in the $D0_3 \leftrightarrow B2$ transition temperature, typically Ti.[6,7]
- Strengthening by coherent precipitates—the most effective way to enhancing the HT properties, typically for Ti.[8]
- Strengthening by incoherent precipitates—typically Zr, Nb, or Ta.[9,10]

The number of additives with proper solubilities in Fe₃Al iron aluminide is not high. The effect of Cr, Ti, V, Mo, Si, and Mn on the value of the 0.2 pct yield stress is described in detail in References 4, 5 and 11 through 14. References 4 and 11 are the first effort to describe the value of 0.2 pct proof stress in iron aluminide with the use of the Labusch's theory of SSH.[15] Recently, Kratochvíl *et al.*[5] have measured and discussed the combined effect of two solutes in an iron aluminide and compared it to the effect of a single solute. The additivity of the strengthening effects of single solutes

PETR KRATOCHVÍL, JOSEF PEŠIČKA, PETER MINÁRIK, and ROBERT KRÁL are with the Department of Physics, Faculty of Mathematics and Physics, Charles University, Ke Karlovu 5, 12116 Prague 2, Czech Republic. Contact e-mail: pekrat@met.mff.cuni.cz STANISLAV DANIŠ is with the Department of Condensed Matter Physics, Faculty of Mathematics and Physics, Charles University, Ke Karlovu 5, 12116 Prague 2, Czech Republic.
Manuscript submitted February 22, 2018.
Article published online September 17, 2018.

was tested. There were found higher values than the sum of the solid solution strengthening contributions by individual solutes in the case of concentrations above ~ 5 at. pct. The explanation was based on the structural ordering that appeared in the alloys.

In this study, the effect of high concentrations of V and Cr in Fe_3Al on the microstructure and mechanical properties is studied. The data available in the Landolt–Bernstein ternary diagrams (Springer Materials)[16] indicate that the solid solubility of both Cr and V in the Fe corner of Fe-Al-Cr and Fe-Al-V ternary diagrams is sufficiently high enough to increase V and Cr concentration in Fe_3Al up to 25 at. pct of both. Therefore, the main goal is to explore the possible increase in the HT strength of highly alloyed Fe_3Al and to extend the knowledge about the further development of the strength and structure when alloying iron aluminide with even higher concentrations of Cr and V.

In the case of higher concentrations of both solutes, the material has a character of a multi-component material; in such case, it is not possible to define the solvent and solute atoms as in Labusch's theory of SSH. Nevertheless, several authors suggested how to evaluate SSH for HEAs.[17–23]

II. EXPERIMENTAL MATERIAL AND METHODS

A set of iron aluminide alloys with the chemical composition shown in Table I was prepared by the Department of Foundry Engineering, The University of Technology, Brno. The ingots were cast under vacuum using an induction furnace with intensive stirring during melting. The subsequent cooling took place in an argon atmosphere. The chemical composition of all the samples was measured by an energy-dispersive X-ray analysis (EDX) in a scanning electron microscope (SEM) from sufficiently large area—larger than 2×2 mm². At least three measurements were performed for each sample. For several samples, a wet chemical analysis was performed to verify the results acquired by EDX. The mean concentration of the technological impurities coming from the metals used for the preparation of the alloys was as follows: 0.1 at. pct Cr, 0.01 at. pct B, 0.1 at. pct Mn, 0.06 at. pct C (wet chemical analysis).

Table I.   Composition of Investigated Iron Aluminides in Atomic Percent

	Fe	Al	V	Cr
FA-10-10	61.0	18.7	10.2	10.1
FA-12-12	58.4	18.1	11.8	11.7
FA-14-14	52.2	18.6	15.3	13.9
FA-20-20	45.3	15.0	20.0	19.7
FA-25-25	37.9	11.7	25.2	25.2
FA-10-18	54.2	16.6	11.2	18.0
FA-15-25	45.5	14.2	15.1	25.2

Microstructure of the samples was thoroughly investigated by the SEM Zeiss Auriga Compact equipped with an EDAX EDX detector and transmission electron microscope (TEM) JEOL 2000FX. The samples for the SEM were mechanically ground and polished with diamond and alumina suspensions with a decreasing grain size to 0.05 μm. The samples for the TEM were electrochemically prepared by the twin-jet polisher Struers Tenupol 5 in the solution of 20 pct HNO_3 in methanol at 243 K (− 30 °C).

The crystalline structure of the bulk and powdered samples was studied by means of X-ray diffraction (XRD). A Seifert XRD7 diffractometer equipped with a cobalt X-ray tube (Co $K_{\alpha 1}$ = 1.788965 Å, Co $K_{\alpha 2}$ = 1.79285 Å, U = 40 kV, I = 30 mA) was employed. A scintillation counter equipped with a secondary graphite monochromator was used to collect the diffracted rays. The bulk samples for the XRD investigation were prepared similarly as for SEM.

Compression deformation tests were carried out using the deformation device Instron 1186R at a temperature of 1073 K (800 °C) with the initial strain rate of 1.5×10^{-4} s^{-1}. The temperature of 1073 K (800 °C) was chosen because this temperature is well above the yield strength anomaly, which is an unusual increase in the strength with the increasing temperature, typically observed for Fe_3Al iron aluminide-based alloys with a maximum in the temperature range 773 K to 873 K (500 °C to 600 °C).[1] The temperature was kept within the accuracy of 3 K. Samples with dimensions of $5 \times 5 \times 8$ mm³ were prepared by electrical discharge machining.

III. RESULTS AND DISCUSSION

It was shown that a high value of the strength at 1073 K (800 °C) of the iron aluminide with 10 at. pct V and 10 at. pct Cr (here, FA-10-10) is connected to the $D0_3$ structure, which was stabilized by V and Cr.[5] Nevertheless, the effect of further increasing the V and Cr content on the microstructure and mechanical properties is unknown. Therefore, a set of iron aluminide alloys with an increasing content of V and Cr was prepared in order to investigate the effect of a symmetric increase of V and Cr (FA-10-10, FA-12-12, FA-14-14, FA-20-20, FA-25-25) and a non-symmetric increase also, in which the increase in the total amount of alloying elements is the same as for the symmetric ones (FA-10-18, FA-15-25).

A. Microstructure

The microstructure of all the investigated alloys was comparable—large grains with a diameter of ~ 350 μm, see Figure 1(a)—larger than 2×2 mm². At least three measurements were performed for each sample. All materials were in the solid solution condition without any major chemical inhomogeneity. A very small fraction of small black particles identified as V_xCr_{1-x} ($0.8 < x < 1$) by TEM (Figure 3) were present in all the alloys. The volume fractions of the observed particles

were calculated from the surface fraction of the particles analyzed by automatic image recognition in ImageJ software from several high-resolution SEM micrographs. The relative volume fraction of these particles was smaller than 1.2 pct in all the investigated alloys; therefore, its effect on mechanical properties can be neglected. No differences in the microstructure between the symmetric and non-symmetric alloys were observed.

XRD investigation was performed in order to analyze crystallographic structure of the alloys. The typical crystallographic structure of iron aluminides at room temperature is $D0_3$—FCC lattice with *Fm-3m* space group. The microstructure of all the investigated alloys consisted of large grains; therefore, it was experimentally impossible to acquire a full XRD profile. As a result, separate scans along the ω and ω–2θ angles were conducted in order to find grains in the diffraction condition with indices {111}, {200}, and {220}, see Figure 2. Note, that the Seifert XRD7 diffractometer is not equipped with a four-circle Eulerian cradle and, consequently, we were not able to align the grains within the sample into the diffraction condition with high accuracy. As a result, the XRD profile peaks are not aligned on precise positions, but it was proven that all

the investigated alloys had a $D0_3$ crystallographic structure.

A detailed observation of the microstructure using the TEM was performed to extend the investigation of the crystallographic structure and to precisely identify the secondary phase particles observed in all the samples. The TEM micrograph presented in Figure 3(a) shows both the matrix and also the detail of the dark particle shown in Figure 1(b). The selected area electron diffraction (SAED) analysis of this material showed that the matrix is ordered in a BCC structure with FCC symmetry, which corresponds to $D0_3$. Figure 3(b) shows the diffraction pattern of the [110] zone. Thus, the results of the TEM analysis are consistent with XRD as shown above. The material was studied with the TEM equipped with EDX. The structure was determined on the basis of electron diffraction (see Figure 3). The composition of the particles was evaluated on the basis of the EDX analysis. Most particles contain pure vanadium or vanadium with a very low concentration of chromium. All the EDX results are from the interval of the compositions, which correspond to the V_xCr_{1-x} particles ($0.8 < x < 1$, $a = 3.02$ Å), see Figure 3(c).
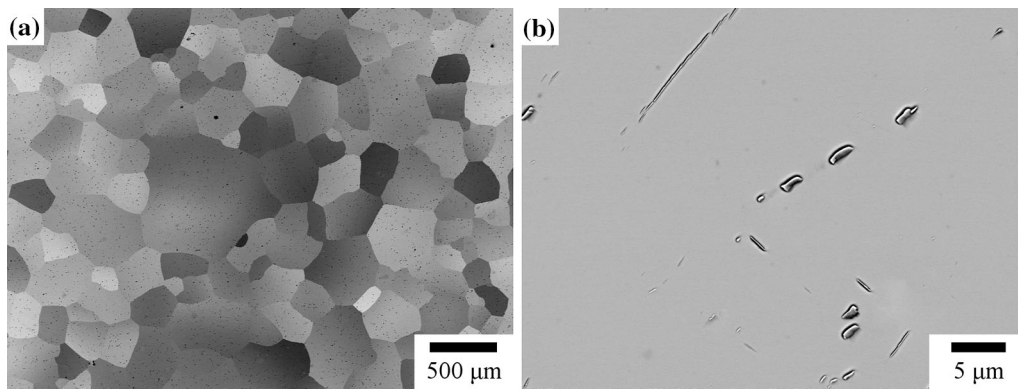

Fig. 1—Microstructure of the FA 14-14 sample—(*a*) overview and (*b*) detail of V_xCr_{1-x} ($0.8 < x < 1$) particles.
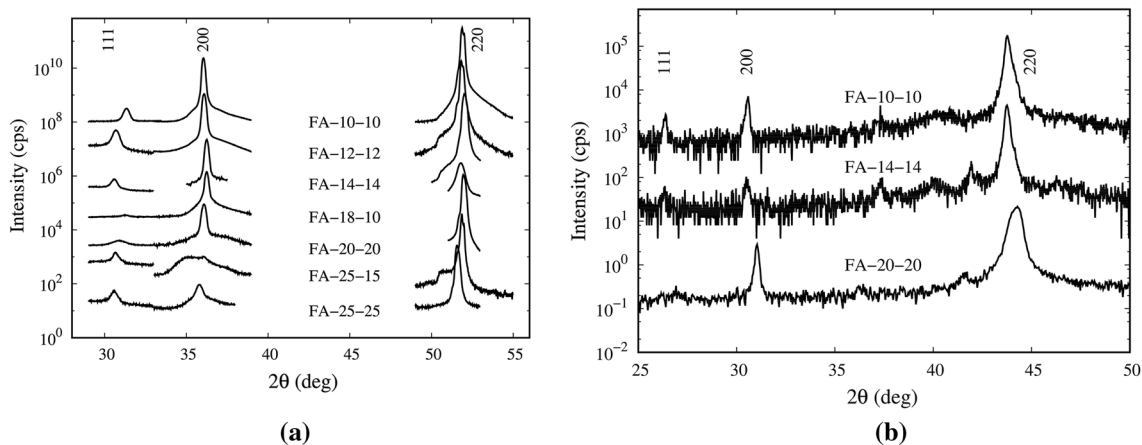

Fig. 2—(*a*) XRD patterns of bulk samples measured using Co K_α radiation at room temperature. (*b*) XRD measured at 1073 K (800 °C) of selected samples using Cu K_α radiation. Diffraction lines with indices {111}, {200}, and {220} proving $D0_3$ structure are clearly visible.
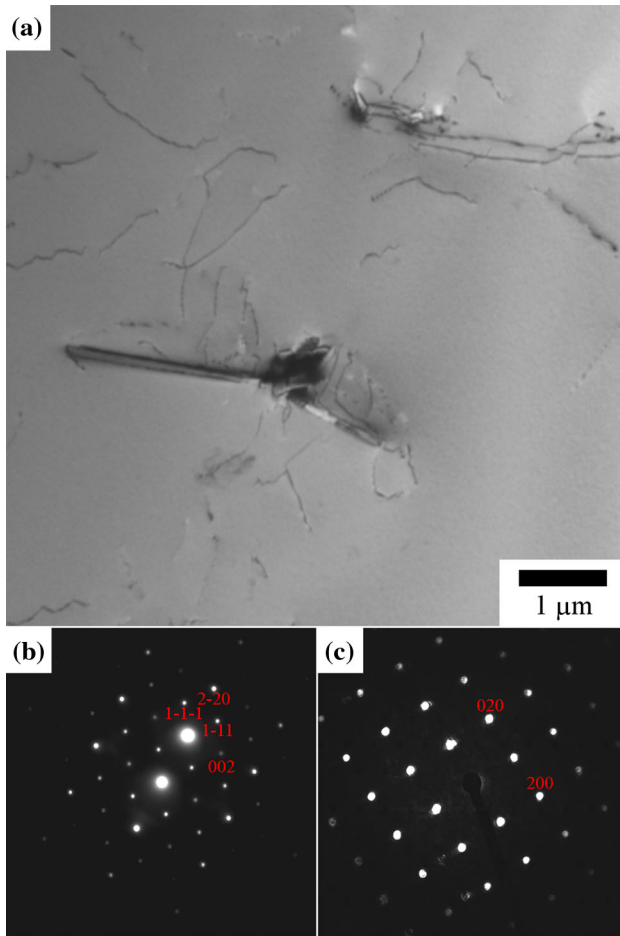
Fig. 3—(*a*) TEM image in bright field mode of FA-20-20 material with diffraction patterns, (*b*) SAED pattern of the matrix—pole [110], (*c*) SAED pattern of V_xCr_{1-x} (0.8 < x < 1) particle—pole [001].

Fig. 4—Lattice parameter evolution as a function of alloying elements concentration for symmetric alloys.

Beside the overall crystallographic structure of the investigated alloys, the lattice parameters for the individual materials were analyzed by the Rietveld method as well.[24] This analysis was performed particularly in order to investigate the evolution of the lattice parameters as a function of the alloying elements concentration. The corresponding results are shown in Figure 4. The dashed line corresponds to a linear regression with a slope of $a = 0.0011(2)$ Å/at. pct and an intercept of $b = 5.792(7)$ Å. The solid line shows the linear dependence of the lattice parameter using Vegard's law for the solid solution of two phases—Fe_3Al and $Cr_{0.5}V_{0.5}$. The latter crystallizes within the BCC structure. In order to keep the FCC lattice, we have used double the value of the lattice parameter $a_{Cr_{0.5}V_{0.5}} = 2a_{BCC} = 5.896$ Å.[13] Consequently, the dependence of the lattice parameter on the Cr and V atomic concentration can be expressed as [1].

$$a = (1 - 2x)a_{Fe_3Al} + 2xa_{Cr_{0.5}V_{0.5}}. \quad [1]$$

For $a_{Fe_3Al} = 5.7911$ Å, we obtain slope $a = 0.00105$ Å/at. pct and intercept $b = 5.7911$ Å, which is very close to the previous linear regression. It
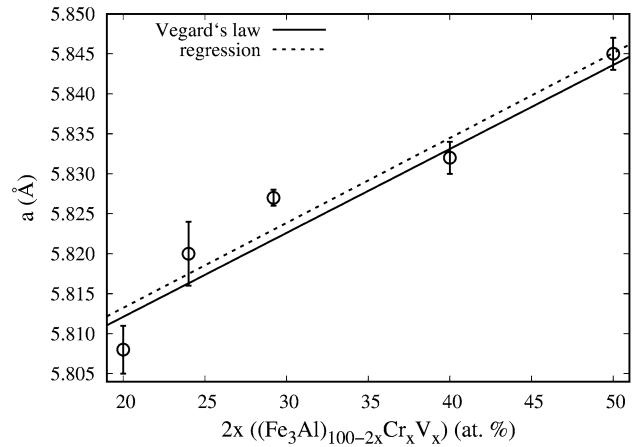
should be noted that the non-symmetric alloys were excluded from this plot. The main reason was that the assumption of the binary alloy consisting of Fe_3Al and $Cr_{0.5}V_{0.5}$ failed for these materials and considering the true ratio in Cr_xV_{1-x} did not lead to trustworthy results. A similar effect, but significantly smaller, was observed for FA-14-14 also. This alloy had a higher concentration of V than preferred, see Table I. Consequently, the measured data failed to follow Vegard's law within the experimental error, see Figure 4. Further investigation in this regard is ongoing in order to fully understand the effect of non-symmetric concentrations on the lattice occupancy.

As known, the $D0_3$ structure has limited thermal stability in the case of pure Fe_3Al.[1] Therefore, the thermal stability of the observed $D0_3$ structure was investigated in all the studied alloys at temperatures up to 1073 K (800 °C). *In situ* annealing in a HT MRI TC-Basics chamber installed in a Panalytical X'Pert MPD diffractometer was performed. The measurement was conducted with Bragg–Brentano geometry using Cu K_α radiation. The diffracted rays were detected using a gas-filled proportional detector equipped with a graphite monochromator. A constant irradiated area of 3×5 mm^2 was held during the measurements using automatic divergence slits. The structure of all the investigated samples remained at $D0_3$ up to 1073 K (800 °C). The diffraction patterns are depicted in Figure 2(b) for selected samples, where lines 111, 200, and 220 are marked in order to prove the existence of the $D0_3$ phase.

B. *Mechanical Strength*

The results of the mechanical strength investigation by the compression deformation tests at 1073 K (800 °C) are summarized in Table II. It is clear that the compressive yield stress significantly increases with the increasing content of the alloying elements (Cr and V). The microstructure investigation did not reveal any significant change in the grain size or the secondary particles volume fraction; therefore, it allows us to

Table II. Compressive Yield Stress of Investigated Alloys Measured at 1073 K (800 °C)

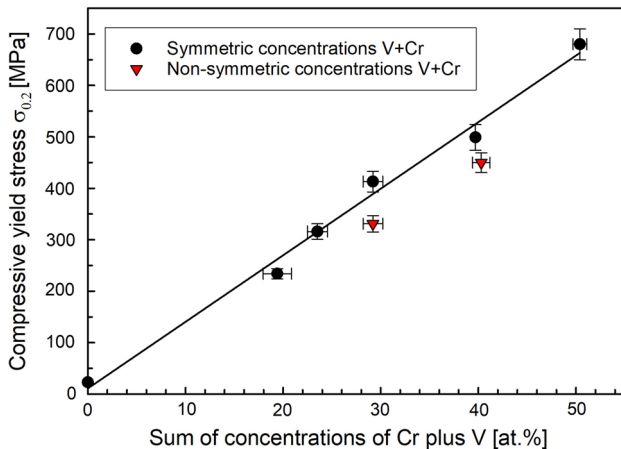| Alloys	Yield Stress (MPa)
FA-10-10	234 ± 8
FA-12-12	316 ± 12
FA-14-14	413 ± 16
FA-20-20	499 ± 19
FA-25-25	680 ± 24
FA-10-18	331 ± 16
FA-15-25	450 ± 19

Fig. 5—Dependence of compressive yield stress on total sum of concentration Cr plus V. Yield stress of unalloyed Fe₃Al was taken from Reference 1.

evaluate these results with respect to the concentration of the alloying elements, see Figure 5.

The results in Figure 5 clearly depict that there is a linear dependence between the compressive yield stress and the sum of the concentration of V plus Cr; nevertheless, this only holds for the symmetric alloys. The non-symmetric alloys with the same total sum of alloying elements have significantly lower yield stress than their symmetric counterparts.

The microstructural investigation, and especially the investigation by XRD, revealed that the microstructure of all the studied alloys has a $D0_3$ order, which is stable even at a HT (1073 K, 800 °C). For this case, the concept of explaining the solute strengthening of medium entropy alloys (MEAs)[25] using the model of Labusch[15] (dilute alloys with non-interacting solutes) is not suitable. In the following section, we formulate a hypothesis on which basis we will conduct our further research on the MEAs derived from iron aluminides.

It should be noted that the XRD analysis revealed that for the symmetric alloys, there is a good agreement with Vegard's law, see Figure 4, and there is also a linear relation between the compressive yield stress and the total sum of Cr plus V. According to Eq. [1], one can suppose that two sublattices (for Fe-Al and Cr-V) with four different atomic occupations exist in the investigated samples. A connection between the four sub-cells

in the $D0_3$ structure could be expected. Increasing the concentration of the V and Cr components results in a more equal occurrence of each element in the alloy. The presence of the Fe₃Al "component" can be the reason why the order is introduced into this series of alloys.

Consequently, the situation approaches the possibility that each of the four sub-lattices is occupied by one type of component and, thus, a higher strength for a higher order is reached. The possibility to strengthen iron aluminides by the order, in fact by keeping the $D0_3$ structure, even at HTs was shown by Palm,[4,26] who increased the temperature of the $B2/D0_3$ transition by alloying Ti and found a comparably high yield stress at HTs. In the case of non-symmetric alloys (with unequal concentration of V and Cr), a more random occupation of the lattice positions would be expected and, as a result, a lower ordering in the alloy caused a decrease in the alloy strengths compared to the symmetrical counterparts, as shown in Figure 5.

The other possible explanation of the observed compression yield stress increase is a theory, which was originally formulated for high entropy alloys by Varvenne et al.[20] The investigated FA-20-20 and FA-25-25 alloys could be, in fact, considered as a case for which this theory could be applied. This model is based on the idea that solute strengthening at an arbitrary solute concentration is an approximation of solutes in an effective matrix. The strengthening arises from the interactions between the solutes and the individual dislocations during slip. The interaction energy for any dislocation in the matrix depends on the precise configuration of the solutes in its vicinity. In addition, the magnitude of the changes of the potential energy and the associated standard deviation are directly connected to the flow stress increase. During the dislocation motion through a random field of solutes, dislocations tend to form a minimum energy wave configuration. This configuration is characterized by the lateral length and amplitude of the wave segments along the dislocation line. Consequently, the characteristic lateral length would increase with the increasing concentration of the solutes; therefore, the compressive yield stress would increase, as observed in Figure 5. This theory[20] does not explain the different values in the compressive yield stress observed for the symmetric and non-symmetric alloys with the same total sum of V plus Cr. Therefore, the idea of a long-period ordering and formation of sub-lattices within the matrix is more adequate for the measured data in this study.

As regards the influence of the individual elements, previous investigation of the effect of low concentrations of Cr and V solutes on HT strengthening in Fe₃Al has shown a very low effect of Cr atoms compared to V atoms.[5] This can be attributed to the differences of respective misfit parameters according to the Labusch's model of solid solution strengthening.[15] The situation changes if the concentrations of Cr and V increase and alloying atoms become a part of an ordered lattice. This was observed in one of the alloys in Reference 5. The important result of the present paper is the tests of seven different alloys which show that the increase of HT strength of Fe₃Al alloyed by high concentrations of Cr

and V is connected to their ordered structure. The strengthening is higher for equal concentrations of Cr and V compared with alloys which have higher concentration of Cr than V. In the latter case, the V atoms are replaced in their positions by Cr atoms which makes the ordered lattice weaker.

The composition of the FA-25-25 alloy is (at. pct) 38 pct Fe-12 pct Al-25 pct Cr-25 pct V, which is close to the MEA alloy 25 pct Fe-25 pct Al-25 pct Cr-25 pct V, in which the tendency of $D0_3$ ordering was also observed in Reference 27.

IV. CONCLUSIONS

Eight iron aluminide alloys with different contents of V and Cr were prepared. The effect of the V and Cr concentration on the microstructure and mechanical properties was investigated:

- The microstructure of all the investigated alloys was comparable, regardless of their chemical composition. In all the alloys, the grain size was ∼ 350 μm, the crystallographic structure was $D0_3$. A small volume fraction of the V_xCr_{1-x} (0.8 < x < 1) small particles was present, without any effect on the strength of the studied alloys.
- XRD measurements proved that the $D0_3$ structure is stable up to 1073 K (800 °C).
- The compressive yield stress significantly increased with the increasing total sum of V plus Cr. Much higher values of the yield stress were measured for the symmetric concentrations of V and Cr when compared to the non-symmetric compositions with more Cr than V.
- The formation of at least a rough system of the lattice positions occupation by four types of atoms in four sub-lattices derived from $D0_3$ was considered as a major strengthening factor for the alloys with the symmetric concentration of V and Cr.

ACKNOWLEDGMENT

REFERENCES

1. C.G. McKamey: in *Physical Metallurgy and Processing of Intermetallic Compounds*, N.S. Stoloff and V.K. Sikka, eds., Chapman and Hall, New York, 1996, p. 351.
2. N.S. Stoloff: *Mater. Sci. Eng. A*, 1998, vol. 258, pp. 1–14.
3. D.G. Morris and M.A. Muñoz-Morris: *Mater. Sci. Eng. A*, 2007, vol. 462, pp. 45–52.
4. M. Palm: *Intermetallics*, 2005, vol. 13, pp. 1286–95.
5. P. Kratochvíl, R. Král, S. Daniš, J. Pešička, and P. Minarik: *Metall. Mater. Trans. A*, 2017, vol. 48A, pp. 4135–39.
6. M. Palm and J. Lacaze: *Intermetallics*, 2006, vol. 14, pp. 1291–1303.
7. R. Krein and M. Palm: *Mater. Sci. Eng. A*, 2007, vols. 460–461, pp. 174–79.
8. I. Jung and G. Sauthoff: *Z. Metallkde*, 1989, vol. 80, pp. 484–89.
9. F. Stein, G. Sauthoff, and M. Palm: *Z. Metallkde*, 2004, vol. 96, pp. 469–85.
10. A. von Keitz, G. Sauthoff, and P. Neumann: *Z. Metallkde*, 1998, vol. 89, pp. 803–06.
11. P. Kratochvil, J. Pešička, R. Král, M. Švec, and M. Palm: *Metall. Mater. Trans. A*, 2015, vol. 46A, pp. 5091–94.
12. R. Prescott and M.J. Graham: *Oxid. Met.*, 1992, vol. 38, pp. 73–87.
13. K. Vedula: in *Intermetallic Compounds, Practice*, J.H. Westbrook and R.L. Fleischer, eds., Wiley, Chichester, 1995, vol. 2, p. 199.
14. M.G. Mendiratta: *Mater. Res. Soc. Symp. Proc.*, 1987, vol. 81, pp. 393–404.
15. R. Labusch: *Phys. Status Solidi*, 1970, vol. 41, pp. 659–69.
16. *Landolt–Börnstein Ternary Alloy Systems: Phase Diagrams, Crystallographic and Thermodynamic Data*, 2nd ed., G. Effenberg, and S. Ilyenko, eds., *Landolt–Börnstein Ternary Alloy Systems: Phase Diagrams, Crystallographic and Thermodynamic Data*, Springer, Berlin, 2008.
17. I. Toda-Caraballo and P.E.J. Rivera-Díaz-del-Castillo: *Acta Mater.*, 2015, vol. 85, pp. 14–23.
18. I. Toda-Caraballo, J.S. Wróbel, S.L. Dudarev, D. Nguyen-Manh, and P.E.J. Rivera-Díaz-del-Castillo: *Acta Mater.*, 2015, vol. 97, pp. 156–69.
19. I. Toda-Caraballo: *Scripta Mater.*, 2017, vol. 127, pp. 113–17.
20. C. Varvenne, A. Luque, and W.A. Curtin: *Acta Mater.*, 2016, vol. 118, pp. 164–76.
21. O.N. Senkov, J.M. Scott, S.V. Senkova, D.B. Miracle, and C.F. Woodward: *J. Alloys Compd*, 2011, vol. 509, pp. 6043–48.
22. Z. Wang, Q. Fang, J. Li, B. Liu, and Y. Liu: *J. Mater. Sci. Technol.*, 2018, vol. 34, pp. 349–54.
23. N.L. Okamoto, K. Yuge, K. Tanaka, H. Inui, and E.P. George: *AIP Adv.*, 2016, vol. 6, p. 125008.
24. T. Roisnel and J. Rodriguez-Carvajal: in *Materials Science Forum, Proceedings of the Seventh European Powder Diffraction Conference (EPDIC 7)*, R. Delhez and E.J. Mittenmeijer, eds., 2000, pp. 118–23.
25. Z. Wu, Y. Gao, and H. Bei: *Acta Mater.*, 2016, vol. 120, pp. 108–19.
26. M. Palm and G. Sauthoff: *Intermetallics*, 2004, vol. 12, pp. 1345–59.
27. J. Pešička, R. Král, S. Daniš, P. Minárik, J. Veselý, V. Šíma, and J. Šmilauerová: *Mater. Sci. Eng. A*, 2018, vol. 727, pp. 184–91.